Journal of Applied Polymer Science

Tensile mechanical properties and constitutive model for HTPB propellant at low temperature and high strain rate

Zhejun Wang, Hongfu Qiang, Guang Wang, Quanzhang Huang
601 Staff room, Xi'an Hi-Tech Institute, Xi'an 710025, China
Correspondence to: Z. Wang (E-mail: qinglongzaitian888@163.com)

ABSTRACT: To investigate the mechanical properties and fracture mechanisms of hydroxyl-terminated polybutadiene (HTPB) propellant at low temperature and high strain rate, uniaxial tensile tests were conducted over the range of temperatures 233 to 298 K and strain rates 0.4 to 14.14 s^{-1} using an INSTRON testing machine, and scanning electron microscope (SEM) was employed to observe the tensile fracture surfaces. The experimental results indicate that the deformation properties of HTPB propellant are remarkably influenced by temperature and strain rate. The characteristics of stress–strain curves at low temperatures are different from that at room temperature, and the effects of temperature and strain rate on the mechanical properties are closely related to the changes of properties and the fracture mechanisms of HTPB propellant. The dominating fracture mechanism depends much on the temperature and changes from the dewetting and matrix tearing at room temperature to the particle brittle fracture at low temperature, and the effect of strain rate only alters the mechanism in a quantitative manner. Finally, a nonlinear viscoelastic constitutive model incorporating the damage evolution and the effects of temperature and strain rate was developed to describe the stress responses of this propellant under the test conditions. During this process, the Schapery-type constitutive theories were applied and one damage variable was considered to establish the damage evolution function. The overlap between experimental results and predicted results are generally good, which confirms that the developed constitutive model is valid, however, further researches should be done due to some drawbacks in describing the deformation behaviors at very large strain. © 2015 Wiley Periodicals, Inc. J. Appl. Polym. Sci. **2015**, *132*, 42104.

KEYWORDS: composites; mechanical properties; theory and modeling; viscosity and viscoelasticity

Received 3 August 2014; accepted 10 February 2015
DOI: 10.1002/app.42104

INTRODUCTION

The structural reliability of a solid rocket motor (SRM), which serves as the propulsion system and the key component of a tactical missile, is extraordinary important. While the performance of such motor is influenced largely by the mechanical properties of propellant grain.[1] This is because solid propellant is viscoelastic in nature and its mechanical properties and fracture mechanisms are highly temperature and strain-rate (and therefore time) dependent.[2] Therefore, to ensure the structural reliability of SRM for the tactical missile during ignition at low temperatures, it is very important to know the mechanical properties and fracture mechanisms of solid propellant at low temperatures (<253 K) and high strain rates (1–20 s^{-1}).[3–6]

In the past decades, a considerable amount of work has been done to investigate the properties of solid propellant under various loading conditions.[7–9] However, there is still limited information available on the mechanical properties and fracture mechanisms of solid propellant at low temperatures and high strain rates. On the one hand, the existing researches regarding the properties of solid propellant at low temperatures are mainly focus on the effects of components on the mechanical properties[10,11] and the varying of glass transition temperature T_g with the various influencing factors,[12,13] etc. Furthermore, in these researches, the tests are mostly carried out at low strain rates (<1 s^{-1}) and less effort has been spent in trying to analyze the fracture mechanisms of solid propellant at low temperatures. On the other hand, there have been several studies on the dynamic mechanical properties of solid propellant, but they are mostly based on the uniaxial compression tests at very high strain rates (>10^3 s^{-1}) with the split Hopkinson pressure bar (SHPB) apparatus,[14,15] and the strain rate in these studies is much higher than that for many solid propellants of tactical missiles igniting.[5] Furthermore, the effect of strain rate on the tensile mechanical properties and fracture mechanisms of solid propellant at high strain rates almost has never been investigated. The previous researches had indicated that the mechanical properties of solid propellant under dynamic conditions of

Additional Supporting Information may be found in the online version of this article.

loading are significantly different from that measured under static conditions.[16] Moreover, at the same temperature and strain rate, it is easier for solid propellant to be failure because of the tensile loading, rather than the compressive loading.[17] Therefore, it is necessary to study the tensile mechanical properties and fracture mechanisms of solid propellant at low temperatures and high strain rates.

In recent decades, much attention has been attached to the development of constitutive models which can describe the effects of temperature and strain rate on the properties of the highly particle-filled elastomers.[18–21] However, at present, there is a lack of suitable constitutive model that can effectively describe the mechanical properties of these materials at various temperatures and high strain rates. The related publications in the extant literature are mainly focused on the following researches. Ho[22] proposed a constitutive model for high strain-rate impact loading conditions by incorporating mechanical damage and nonlinear viscoelastic response of solid propellant. However, this model is not suitable to describe the tensile mechanical properties of solid propellants because of the different loading method. Furthermore, it cannot adequately describe the mechanical properties of these materials at low temperatures because of the method considering the effect of temperature. Another model developed by Zhu, Wang, and Tang (ZWT)[23] has been widely used to describe the mechanical properties for a variety of composites over the range of strain rates 10^{-4} to 10^{3} s^{-1}. However, this model cannot describe the mechanical properties of materials over the range of strain rates 1 to 10^{2} s^{-1} and the deformation behaviors of materials at large strain. Wang *et al.*[24] proposed a new damage evolution law and a new fracture criterion to improve the predictive ability of this model, but it is difficult to determine the threshold fracture strain and the deformation behaviors at the strain over 15% still cannot be described by the damage modified ZWT model. Therefore, the more effective method should be proposed to describe the tensile mechanical properties of highly particle-filled elastomers such as solid propellant at low temperatures and high strain rates.

Solid propellant based on hydroxyl-terminated polybutadiene (HTPB) binder is a typical highly particle-filled elastomer and has become the workhorse propellant in present-day SRM worldwide.[25] Therefore, the tensile mechanical properties and fracture mechanisms of HTPB propellant at low temperatures and high strain rates were studied in this investigation, based on the uniaxial tensile tests in a wide range of temperatures and strain rates and electron microscopy scanning on the tensile fracture surfaces. A nonlinear viscoelastic constitutive model incorporating the damage evolution and the effects of temperature and strain rate was developed to describe the stress responses of this propellant under the test conditions. Finally, the validity of the developed constitutive model was examined by comparing the experimental and predicted results.

EXPERIMENTAL

The material used in this investigation was taken from the composite rocket propellant and consists of an 88 wt % mixture of ammonium perchlorate (AP) and fine aluminum particles bound together with 12 wt % of a HTPB polymer binder. Standard JANAF uniaxial tensile samples were tested at temperatures of 233, 243, 253, and 298 K and at constant crosshead rates of 0.40, 1.00, 4.00, and 14.14 s^{-1}. Five replicates were run at each test conditions and all stress–strain curves investigated in the following sections were the average of the five data sets. The samples were stored at the test temperature for an hour prior to testing and were then tested at a constant crosshead rate until they fractured. The test temperatures were determined according to the following reasons. Firstly, it is based on the Chinese aerospace industry standards (for example QJ 1615-89). Secondly, Jeremic[5] had stated that if the real operating conditions of SRM were taken into account, the mechanical properties of solid propellants during ignition of SRM at low temperatures (<253 K) should be mostly studied.

The previous researches had indicated that it is difficult to obtain the stress–strain data of materials under the uniaxial tensile test with SHPB.[26] And when the strain rate is lower than 10^{2} s^{-1}, the test results obtained with the SHPB is not accurate enough due to the properties of this apparatus. Therefore, in this investigation, uniaxial tensile tests were conducted on a classical testing machine INSTRON VHS 160/100-20, which can guarantee the constant crosshead rate up to 20 m/s at temperature interval from −113 K to 973 K and can apply optional thermal loading conditions to the testing sample with a thermal chamber. However, the original gripping method of this testing machine used for metal materials does not work well due to the solid propellant's lower strength. In this investigation, a new set of aluminum gripping jaws was designed and manufactured, as shown in Figure 1. And this new set of jaws has got the patent in People's Republic of China.[27] A Quanta 600FEG SEM was used for routine post-failure examination. Samples were mounted using a conductive paint onto SEM stubs and sputter coated with a thin layer of gold prior to examination.

RESULTS AND DISCUSSION

Stress–Strain Behavior

The stress–strain curves of HTPB propellant at various test conditions are shown in Figure 2 and the characteristics are represented as follows:

1. The deformation behaviors of HTPB propellant are remarkably influenced by temperature and strain rate. And the stress increases significantly when decreasing temperature and increasing strain rate. Furthermore, the HTPB propellant is capable of large deformation and displays nonlinear material behavior, which is usually associated with the occurrence of the damage in the propellant during the tensile deformation.[28]
2. The stress–strain curves exhibit two different shapes at various test temperatures, as shown in Figure 3. There are three common regions in the stress–strain curves at room temperature, which is (I) the linear elastic region, (II) the metal like hardening region, and (III) the failure region, respectively. Whereas at low temperatures, there are five regions, which is (I) the linear elastic region, (II) the metal like hardening

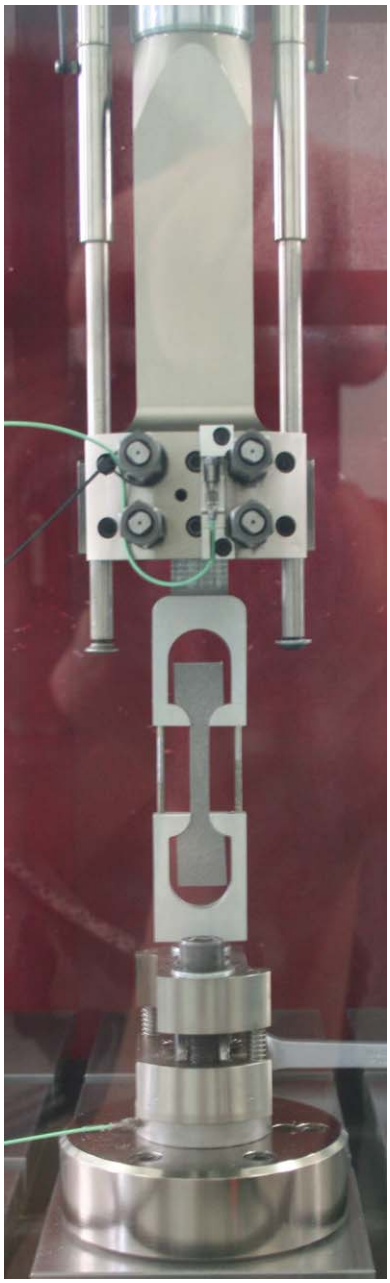

Figure 1. Standard JANAF uniaxial HTPB propellant tensile sample and the new designed aluminum gripping jaws with the tensile testing machine INSTRON VHS 160/100-20 in place. [Color figure can be viewed in the online issue, which is available at wileyonlinelibrary.com.]

region, (III) the strain softening region, (IV) the strain hardening region, and (V) the failure region, respectively. In addition, Figure 2 shows that it is easier for the stress–strain curve to shown these five regions at lower temperature and higher strain rate.

In this investigation, the characteristic of stress–strain curve at low temperature may be caused by the following reasons. Firstly, the propellant may be in glass transition state at the lowest temperature and higher strain rates. Because the glass transition temperature T_g for HTPB propellant is about 203 K, which was detected at the frequency of 3.5 Hz by using dynamic mechanical analysis (DMA) method on a DDV-II-EA testing machine in the range of 173 to 373 K with a heating rate of 1 K/min. And the T_g value appeared to rise approximately 3.5 K as the strain rate was increased by an order of magnitude. Secondly, the fracture mechanisms of HTPB propellant may be more severe and complex at lower temperatures and higher strain rates.

Mechanical Properties and Fracture Mechanisms

Due to the complex characteristics of stress–strain curves for HTPB propellant, the previous method[29] determining the mechanical parameters of highly particle-filled elastomers cannot be effective. In this investigation, based on the method to determine the mechanical parameters of nonmetallic materials,[30] the yield stress σ_0, the associated strain ε_0, and elasticity modulus E were identified on the stress–strain curves in terms of a 1% offset in the total strain, as illustrated in Figure 3. Other parameters were directly obtained on the stress–strain curves, as illustrated in Figure 3.

Figure 4 shows the relationship curves of the mechanical parameters with strain rate at various test temperatures. As shown in Figure 4, the yield stress σ_0, maximum tensile stress σ_m, and elasticity modulus E increase gradually with decreasing temperature and increasing strain rate, and all present linear-log relationships with strain rate at various temperatures. However, the yield strain ε_0 is almost 8% and approximately constant with variations of temperature and strain rate. The strain at maximum tensile stress ε_m decreases as the temperature decreases. When increasing strain rate, the strain ε_m increases at room temperature and decreases at low temperatures as a whole.

The effects of temperature and strain rate on the above mechanical parameters are closely related to the changes of properties and the different fracture mechanisms for HTPB propellant at various temperatures and strain rates.

Firstly, because the propellant becomes stiffer and behaves in a brittle manner at low temperature, the tensile stress and elasticity modulus E increase as the temperature decreases, while the associated strain ε_m decreases.

Secondly, the yield strain ε_0 is usually as the critical strain for dewetting of solid propellant and varies with temperatures and strain rates. However, the typical fractured surfaces of the deformed samples obtained at various test conditions are shown in Figure 5, from which it can be seen that the dominating fracture mechanism of HTPB propellant depends much on the temperature and changes from the dewetting and matrix tearing at room temperature to the particle brittle fracture at low temperature, and the effect of strain rate only alters the mechanism in a quantitative manner. Therefore, the reasons causing the yield of HTPB propellant in this investigation may be not only the dewetting, but also other factors such as nonlinear time-temperature effect and particle rearrangement, etc. The coupled effects of all these mechanisms may be the cause for the independence of the yield strain ε_0 on temperature and strain rate.

Thirdly, at room temperature, microcracks usually initiate in the matrix due to the stress concentration and subsequently

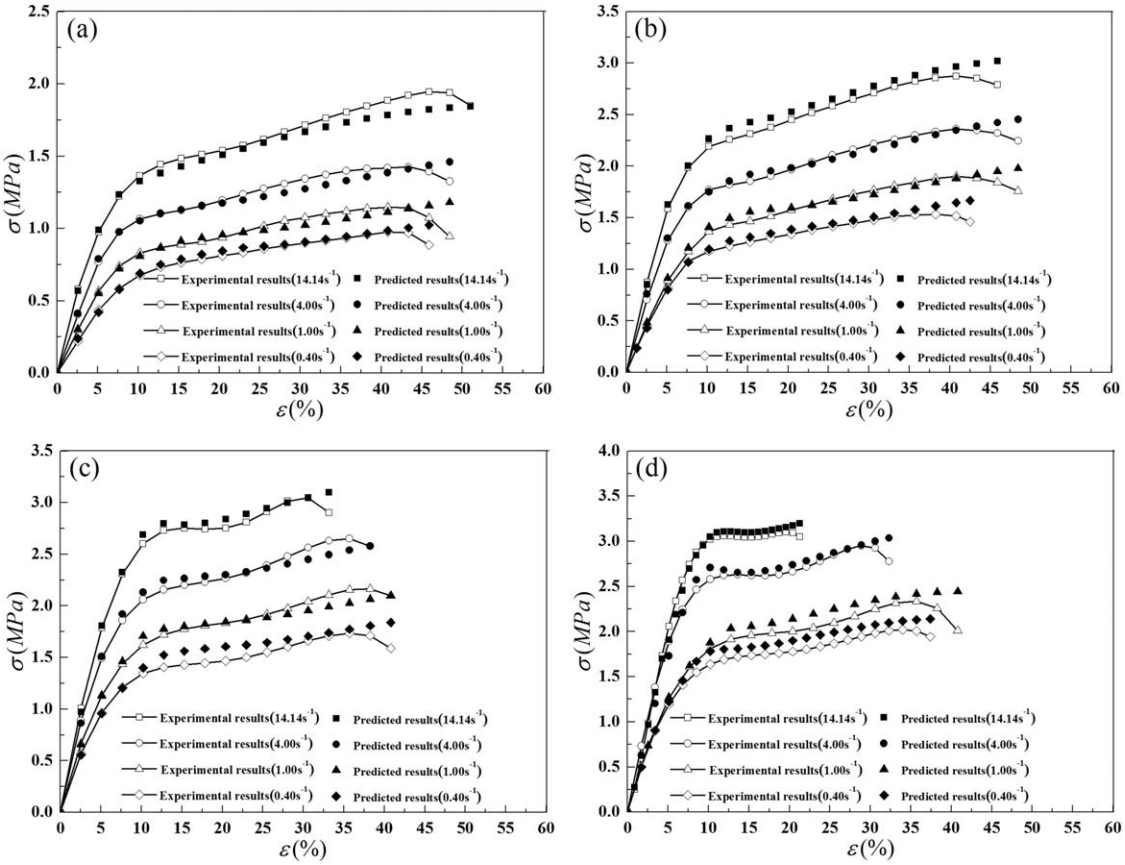

Figure 2. Stress–strain curves of the uniaxial tensile test for HTPB propellant at various temperatures and strain rates (a) 298 K; (b) 253 K; (c) 243 K; (d) 233 K.

propagate in matrix itself or to the interface between the particles and matrix. However, it needs enough time to finish the second process.[31] Therefore, at very high strain rate, there is no enough time for microcracks to propagate to the interface and the microcracks mainly grow, nucleate and propagate in the matrix itself, causing the fracture of the propellant in the form of matrix tearing and the slighter dewetting [Figure 5(b)]. Because the damage of HTPB propellant is slighter at room

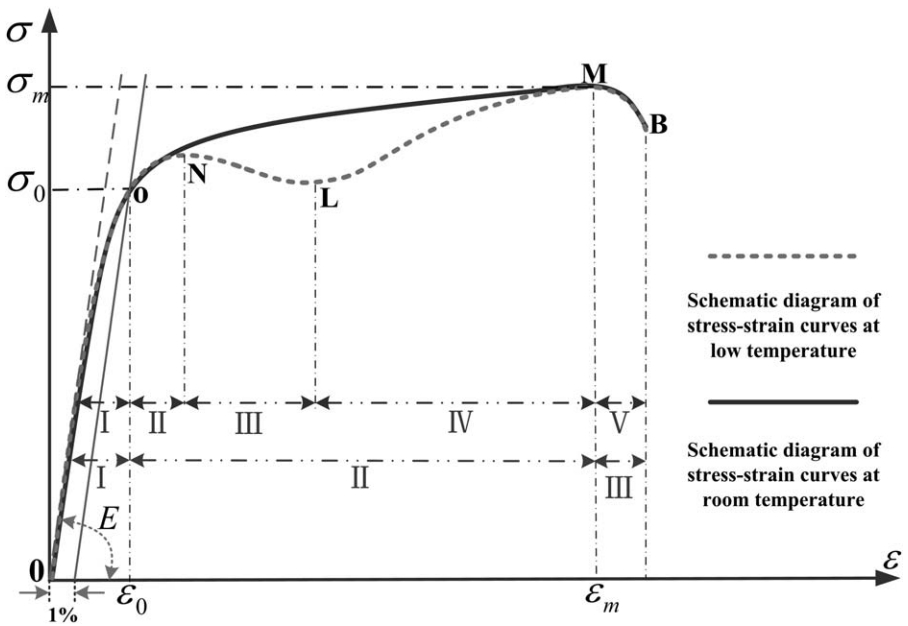

Figure 3. Schematic diagram of stress–strain curves for HTPB propellant at various test temperatures.

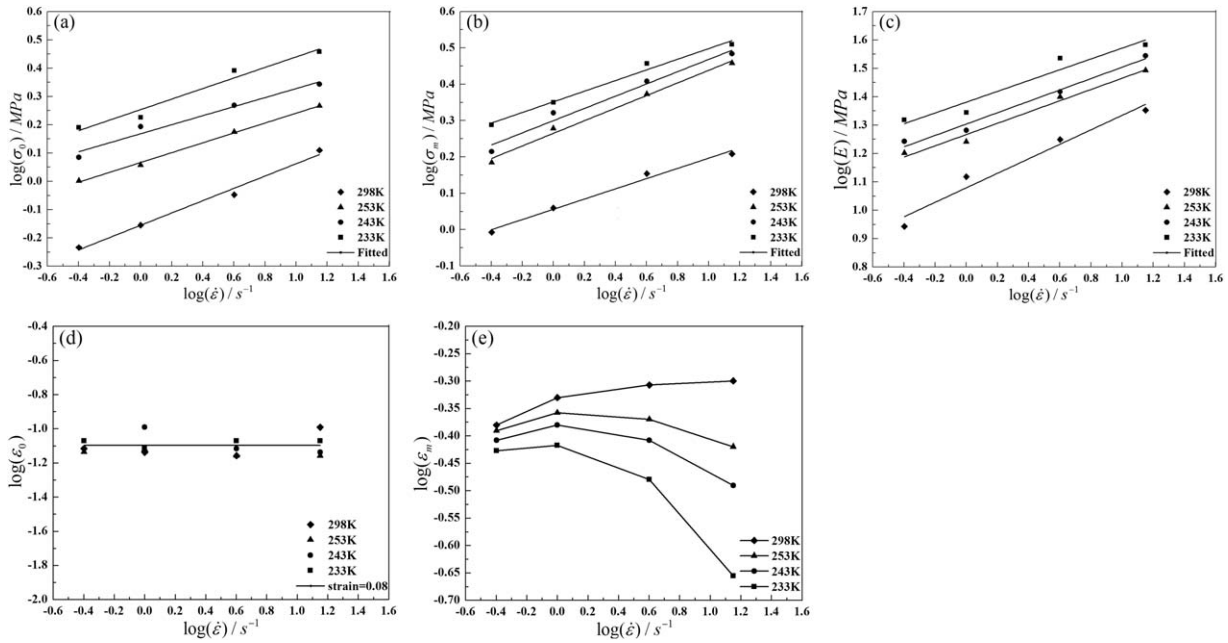

Figure 4. Mechanical parameters of HTPB propellant (a) yield stress; (b) the maximum tensile stress; (c) elasticity modulus; (d) yield strain; (e) strain at maximum tensile stress versus logarithmic strain rate at various test temperatures.

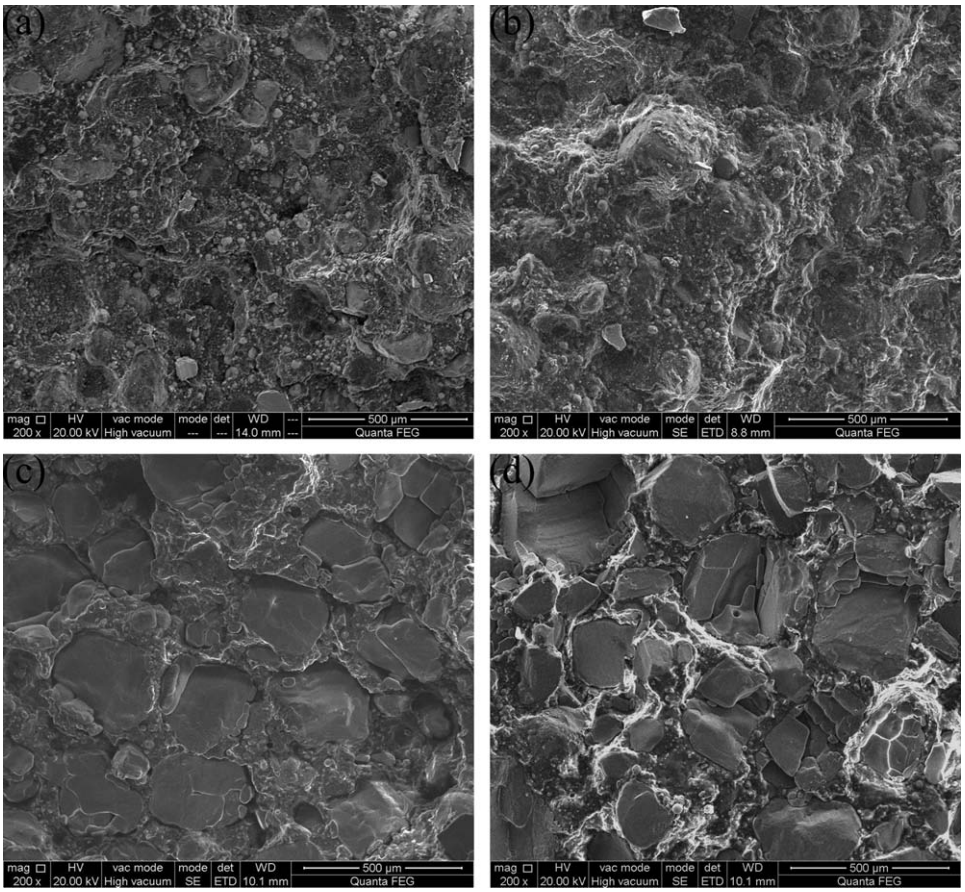

Figure 5. SEM images of the tensile fracture surfaces for HTPB propellant at various temperatures and strain rates (a) 298 K and 0.4 s^{-1}; (b) 298 K and 14.14 s^{-1}; (c) 233 K and 0.4 s^{-1}; (d) 233 K and 14.14 s^{-1}.

temperature and higher strain rate, the strain ε_m increases when increasing strain rate.

Fourthly, the debonding stress for highly particle-filled elastomers is usually expressed as follows:[32]

$$\sigma_d^2 = \frac{4E_b\gamma(2+3V)}{3r(1-V)} \quad (1)$$

where E_b is the Young's modulus of matrix, γ is the interfacial fracture surface energy (i.e. energy to create unite area of two debonded surfaces), r is the inclusion radius, and V is the volume fraction of inclusion.

According to eq. (1), the degree of the debonding is determined by the values of E_b and γ when temperature changes. At low temperature, the values of E_b and γ increase because solid propellant behaves in a brittle manner. However, the fracture stress of particles is approximately constant with variation of temperature or the change is very small. Therefore, it is easier for microcracks to initiate, nucleate and grow in the AP particles when decreasing temperature, as shown in Figure 5(c,d). Moreover, there is a stronger stress wave accompanying with the tensile deformation when increasing strain rate at low temperature, which can induce more microcracks initiating in the AP particles and larger amount of AP particles fracturing [Figure 5(d)], etc. Thus, the coupled effects of low temperature and higher strain rate can cause the more severe damage for HTPB propellant, which induces the lower value of the strain ε_m.

CONSTITUTIVE MODEL

Developing the Constitutive Model

According to the previous researches, it is generally accepted that the nonlinear character of the highly particle-filled elastomers is related to the damage inside them. Therefore, the following expression can be used to model the deformation of these materials at various temperatures and strain rates:[33]

$$\sigma = g \cdot f(\varepsilon, t, T) \quad (2)$$

where the function g is applied to calculate the damage evolution, the function $f(\varepsilon, t, T)$ is applied to describe the linear viscoelastic mechanical property, which is usually related to strain ε, time t and temperature T. At present, it is generally accepted to use the Prony series to model the function $f(\varepsilon, t, T)$,[34] while there are different expressions to describe the other function g.[35–37]

There are usually two methods to establish a damage evolution function g.[38,39] One way is to measure the formation and evolution of microdefec in the materials using acoustic emission (AE). Another way directly uses macroscopic variables to establish a damage evolution function. It is very difficult to determine the related parameters with the first method and only under certain experiment conditions, can this method be used. Thus, the second method was applied in this investigation.

During the different constitutive models with the second method, the ones proposed by Hinterhoelzl and Schapery have been widely used to study the properties of mechanical or fatigue for various materials.[34,37,39,40] Because the stress–strain data is all from one-dimensional experiment in this investigation, based on the Schapery-type constitutive theories, the stress responses of HTPB propellant under the test conditions can be described by the following expressions, in which only one damage variable was considered:[39]

$$\varepsilon^R(t) = \frac{1}{E_R}\int_0^t E(\xi-\xi')\frac{\partial\varepsilon}{\partial\tau}d\tau \quad (3)$$

$$\sigma(t) = \frac{\partial W^R}{\partial\varepsilon^R} = E_R C(S)\varepsilon^R(t) \quad (4)$$

$$W^R = \frac{1}{2}C(S)(\varepsilon^R)^2 \quad (5)$$

$$\frac{dS}{dt} = \left[-\frac{\partial W^R}{\partial S}\right]^{\alpha} \quad (6)$$

$$\text{where} \quad \xi(t) = \int_0^t \frac{dt'}{\alpha_T[T(t')]} \quad (7)$$

and $\xi' = \xi(\tau)$. The quantities t, ξ, and α_T are physical time, reduced time, and the time-temperature shift factor, respectively, the parameter α_T reflects the influence of temperature on internal viscosity of HTPB propellant, $\varepsilon^R(t)$ is pseudo strain, E_R is the reference modulus which can be arbitrarily selected (1 MPa in this investigation), $E(\xi-\xi')$ stands for the relaxation modulus, ε is strain, $\sigma(t)$ is the observed stress, W^R is pseudo strain energy density function, $C(S)$ is pseudo stiffness as a function of damage variable S, and α is material parameter which express the damage evolution rate. In the case of constant strain rate $\dot{\varepsilon}$, eq. (3) can be written as:

$$\varepsilon^R(t) = \frac{\dot{\varepsilon}}{E_R}\int_0^t E(\xi-\xi')d\tau \quad (8)$$

Constitutive Parameters Acquirement

(1) The same test sample was used for the stress relaxation as well as the previous tests in this investigation. According to the constant velocity tensile experiment results, we select 0.05 as the strain level for relaxation tests, at which the mechanical property of HTPB propellant still obeys the linear viscoelastic theory. The strain rate was 1 s^{-1}, the temperature levels were selected as 233, 243, 253, and 298 K, each sample was tested only once and each test was repeated at least five times. Each relaxation test was approximately 1000 s in duration.

Based on the time temperature superposition principle (TTSP), the relaxation curves at various test temperatures were shifted horizontally along the logarithmic time axis to the reference temperature of 233 K. Then the shift factors $\log(\alpha_T)$ and the master relaxation curve were obtained, as shown in Figure 6. The master relaxation curve was expressed by Prony series as follows:

$$E(t) = 0.8150 + 8.0695\exp(-t/\tau_1) + 7.7246\exp(-t/\tau_2)$$
$$+6.4100\exp(-t/\tau_3) + 5.0212\exp(-t/\tau_4) + 3.2168\exp(-t/\tau_5)$$
$$+2.2887\exp(-t/\tau_6) + 1.3220\exp(-t/\tau_7) + 0.9680\exp(-t/\tau_8)$$

where τ_i is the relaxation time and was selected in this investigation as follows:

$$\tau_i = 10^{i-3} \quad (9)$$

(2) According to the master relaxation modulus and eqs. (7) and (8), the pseudo strain $\varepsilon^R(t)$ at various temperatures and

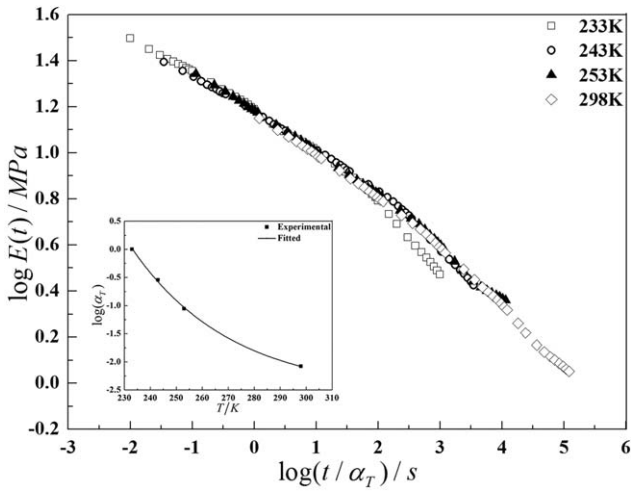

Figure 6. The master relaxation curve reduced to 233 K.

strain rates can be calculated. Then, based on the pseudo strain values and experiment results, the relationships of the parameter $C(S)$ with time t at various temperatures and strain rates can be obtained by eq. (4).

(3) When the damage occurs in HTPB propellant is closely related to the growth of microcracks, the value of α in eq. (6) can be calculated as follows:[41]

$$\alpha = 1 + 1/m \tag{10}$$

where $m \approx -\log E(t)/\log(t)$, $E(t)$ is the relaxation modulus. The damage evolution in eq. (6) is rate-dependent, therefore, the value of α should be independent of strain rate. In this investigation, the initial values of α at various temperatures were determined based on eq. (10) and the relaxation modulus. Then, they were finally obtained by the following process.

Firstly, taking eq. (5) into eq. (6) gives:

$$\frac{dS}{dt} = \left[-\frac{1}{2}\frac{\partial C(S)}{\partial S}(\varepsilon^R)^2\right]^{\alpha} \tag{11}$$

In this investigation, the strain rate is high, so the following incremental relationships can be easily obtained by high data collecting frequency based on eq. (11):

$$\Delta S = \left\{\left[-\frac{1}{2}\Delta C(S)(\varepsilon^R)^2\right]^{\alpha}\Delta t\right\}^{1/(1+\alpha)} \tag{12}$$

$$S_{i+1} \cong S_i + \left\{-\frac{1}{2}[\Delta C(S)]_{i+1}(\varepsilon^R_{i+1})^2\right\}^{\alpha/(1+\alpha)}\Delta t^{1/(1+\alpha)} \tag{13}$$

Based on the initial values of α and the obtained values of the pseudo strain $\varepsilon^R(t)$ and the parameter $C(S)$, the values of S and $S-t$ relationships at various temperatures and strain rates can be obtained by eq. (13). Then, according to $S-t$ relationships and the obtained relationships of the parameter $C(S)$ with time t, the relationships of the parameter $C(S)$ with the variable S at various temperatures and strain rates can be given.

Secondly, at each test temperature, put all of the relationship curves of the parameter $C(S)$ with the variable S at different strain rates in the same coordinate system, then the value of α was adjusted appropriately until the relationship curves of the parameter $C(S)$ with the variable S have a good contact ratio. Now, the final value of α and the final relationship of the parameter $C(S)$ with the variable S at each test temperature were ensured, which are shown in Figures 7 and 8.

(4) Based on the above results, the function $C(S)$ and the relationship of the parameter α with temperature T can be fitted to the forms as follows:

$$C(S) = \frac{\exp(-A_1 S) + \exp(-A_2 S)}{2} \tag{14}$$

$$\alpha(T) = 3.6183 - 6.3152\times10^5 e^{-0.05934T} \tag{15}$$

where the parameters A_1 and A_2 are functions of temperature, and have not physical meanings. The relationship curves of the parameters A_1 and A_2 with temperature T are shown in Figure 8, from which the following fitted expressions can be given:

$$A_1(T) = 0.1438 + 4.1863\times10^{-5} e^{0.02936T} \tag{16}$$

$$A_2(T) = 0.07179 + 0.03183 e^{0.01665T} \tag{17}$$

According to eqs. (14), (16), and (17), the fitting curves of $C(S)-S$ expressed by solid lines at various test temperatures are shown in Figure 7. From Figure 7, it can be seen that the fitting results are good. In this investigation, the effect of temperature on the damage evolution was considered based on the parameters α, A_1, and A_2.

Constitutive Equation Validation

Based on eq. (14), eq. (11) can be written as:

$$\frac{dS}{dt} = \left[\frac{1}{2}\times\frac{A_1\exp(-A_1 S) + A_2\exp(-A_2 S)}{2}(\varepsilon^R)^2\right]^{\alpha} \tag{18}$$

Then, according to eq. (18), the new incremental relationship of damage variable S by high data collecting frequency can be given:

$$\Delta S = \left[\frac{1}{2}\times\frac{A_1\exp(-A_1 S) + A_2\exp(-A_2 S)}{2}(\varepsilon^R)^2\right]^{\alpha}\Delta t \tag{19}$$

$$S_{i+1} = S_i + \left[\frac{1}{2}\times\frac{A_1\exp(-A_1 S_i) + A_2\exp(-A_2 S_i)}{2}(\varepsilon^R_i)^2\right]^{\alpha}\Delta t \tag{20}$$

Based on eqs. (8), (15) to (17) and the master relaxation modulus, the new $S-t$ relationships at various test conditions can be obtained by eq. (20). Then, according to eq. (14), the new functions $C(S)$ at various test conditions were obtained. Finally, according to eqs. (4), (7), and (8) and the master relaxation modulus, the stress responses of HTPB propellant at various test conditions can be predicted.

To verify the developed constitutive model, comparisons between the experimental and predicted results were carried out, as shown in Figure 2. Form Figure 2, it can be obviously found that the overlap between experimental results and predicted results are generally good but some forecast error at very large strain, this is because that there are large scattered errors in HTPB propellant's mechanical properties, which may affect the constitutive parameters accuracy. Besides, as discussed in the previous sections, the characteristics of stress–strain curves and fracture mechanisms for HTPB propellant are very complex at low temperatures and high strain rates. Thus, the more suitable form of the function $C(S)$ should be proposed. To solve

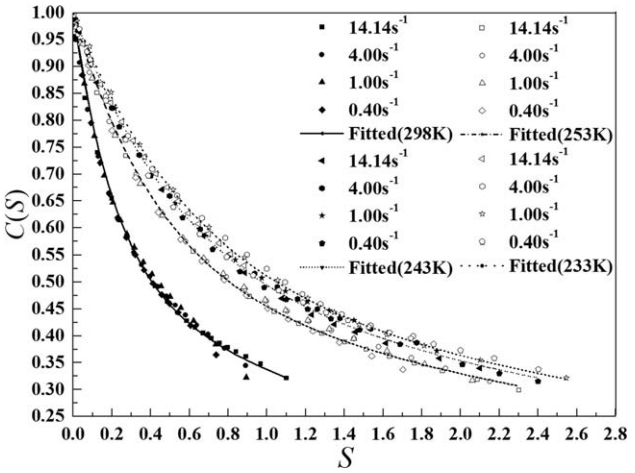

Figure 7. $C(S)$ curves at various test temperatures.

these problems, more effective experimental method and more number of replications should be considered to reduce the negative influence of the large variance, then, according to the amount of experimental results, select the more suitable form of the function $C(S)$ and the more effective method to obtain the constitutive parameters.

CONCLUSIONS

Based on a classical testing machine INSTRON VHS 160/100-20, a new set of aluminum gripping jaws and SEM, the tensile mechanical properties and fracture mechanisms of HTPB propellant at low temperatures and high strain rates were successfully studied. The test method can offer a new effective method for studying the tensile mechanical properties of highly particle-filled elastomers at high strain rates.

HTPB propellant is still capable of large deformation at low temperatures and high strain rates. The stress and elasticity modulus increase with decreasing temperature and increasing strain rate. These properties of HTPB propellant are very important to ensure the structural reliability of SRM during ignition at low temperatures. However, the dominating fracture mechanism of HTPB propellant changes from the dewetting and matrix tearing at room temperature to the particle brittle fracture at low temperature. The coupled effects of the lower temperature and higher strain rate cause more severe and complex damage in the propellant. Furthermore, HTPB propellant may be in glass transition state at the lowest temperature and higher strain rates. Because of these properties of HTPB propellant at low temperatures and high strain rates, the characters of stress–strain curves and mechanical properties of HTPB propellant are different from that at room temperature, which may influence the structural reliability of SRM during ignition at low temperatures. The yield strain ε_0 is almost 8% over the entire range of test conditions, which makes it the critical strain of damage for HTPB propellant at low temperatures and high strain rates. The strain at maximum tensile stress ε_m increases with increasing strain rate at room temperature, while this strain decreases with the coupled effects of lower temperatures and higher strain rates, which indicates that the strain ε_m can be selected as failure criteria for further analysis of the SRM structural reliability during ignition at low temperatures.

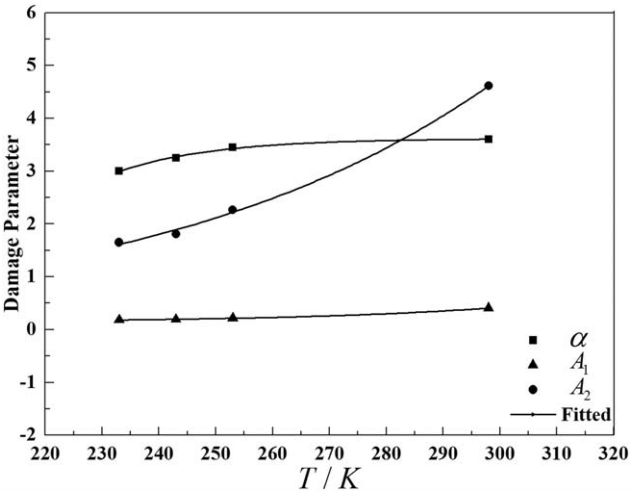

Figure 8. Fitting results of damage parameters α, A_1, and A_2.

A nonlinear viscoelastic constitutive model incorporating the damage evolution and the effects of temperature and strain rate was developed to describe the stress responses of HTPB propellant under the test conditions. During this process, the Schapery-type constitutive theories were applied and one damage variable was considered to establish the damage evolution function. In addition, the constitutive parameters fitting methods were studied on the basis of constant rate tensile tests and relaxation tests. Finally, based on the developed constitutive model and the obtained damage evolution function, the stress responses of HTPB propellant under the test conditions were predicted. The results show that the overlap between experimental results and predicted results are generally good but some forecast error at very large strain, which indicates that the developed constitutive model is valid, but further researches should be conducted.

ACKNOWLEDGMENTS

This research was funded by the National 973 Program in China through grant No. 61338 and 613142.

REFERENCES

1. Goyal, V. K.; Rome, J. I.; Schubel, P. M. Presented at AIAA/ASME/ASCE/AHS/ASC 49th Structures, Structural Dynamics, and Materials Conference; Schaumburg, IL, April 7–10, **2008**.
2. Zalewski, R.; Wolszakiewicz, T. *Cent. Eur. J. Energetic Mater.* **2011**, *8*, 223.
3. Marimuthu, R.; Nageswara Rao, B. *Int. J. Pressure Vessels Piping* **2013**, *111*, 131.
4. Jiang, S. P.; Rui, X. T.; Hong, J.; Wang, G. P.; Rong, B.; Wang, Yan. *Granul. Matter* **2011**, *13*, 611.
5. Jeremic, R. *Propellants Explosives Pyrotechnics* **1999**, *24*, 221.

6. Walley, S. M.; Field, J. E.; Palmer, S. J. P. *Proc. R. Soc. A* **1992**, *438*, 571.
7. Xu, J. S.; Ju, Y. T.; Han, B.; Zhou, C. S; Zheng, J. *Mech. Time Depend. Mater.* **2013**, *17*, 543.
8. Tussiwand, G. S.; Saouma, V. E.; Terzenbach, R.; Luca, L. T. *J. Propul. Power* **2009**, *25*, 60.
9. Chyuan, S. W. *Int. J. Pressure Vessels Piping* **2003**, *80*, 871.
10. Mohamed, A.; Gholamian, F.; Zarei, A. R. *J. Propul. Power* **2014**, *30*, 862.
11. Balzer, J. E.; Siviour, C. R.; Walley, S. M.; Proud, W. G.; Field, J. E. *Proc. R. Soc. A* **2004**, *460*, 781.
12. Hu, C.; Guo, X.; Jing, Y. H.; Chen, J.; Zhang, C.; Huang, J. *J. Appl. Polym. Sci.* **2014**, *16*, 1.
13. De La Fuente, J. L.; Fernández-García, M.; Cerrada, M. L. *J. Appl. Polym. Sci.* **2003**, *88*, 1705.
14. Ho, S. Y.; Fong, C. W. *J. Mater. Sci.* **1987**, *22*, 3023.
15. Kawata, K.; Chung, H. L.; Itabashi, M. *Adv. Compos. Mater.* **1994**, *3*, 163.
16. Herder, G.; Weterings, F. P.; de Klerk, W. P. C. *J. Therm. Anal. Calorim.* **2003**, *72*, 921.
17. Ren, P.; Hou, X.; He, G. R.; Gao, J.; He, T. S. *J Astronautics* **2010**, *31*, 2354.
18. Kakavas, P. A. *Int. J. Solids Struct.* **2014**, *51*, 2019.
19. Deng, B.; Xie, Y.; Tang, G. J. *Propellants Explosives Pyrotechnics* **2014**, *39*, 117.
20. Jardin, A.; Leblond, J. B.; Berghezan, D.; Portigliatti, M. *Procedia Eng.* **2010**, *2*, 1643.
21. Kim, J.; West, R. C. *J. Eng. Mech.* **2010**, *136*, 496.
22. Ho, S. Y. *J. Prop. Power* **2002**, *18*, 1106.
23. Zhou, F. H.; Wang, L. L.; Hu, S. S. *Explosion Shock Waves* **1992**, *12*, 333.
24. Wang, L. L.; Zhou, F. H.; Sun, Z. J.; Huang, D. J. *J NingBo Univ. (NSEE)* **2012**, *25*, 27.
25. De La Fuente, J. L.; Rodríguez, O. *J. Appl. Polym. Sci.* **2003**, *87*, 2397.
26. Siviour, C. R. High Strain Rate Properties of Materials Using Hopkinson Bar Techniques. Ph.D. Thesis; University of Cambridge: England, **2005**.
27. Qiang, H. F.; Wang, G.; Wu, W. M.; Zhang, K. P.; Wang, X. R.; Zhou, S.; Wang, Z. J.; Han, Y. W. P. R. C Pat. ZL 201320,012,760.5, **2013**.
28. Jung, G. D.; Youn, S. K.; Kim, B. K. *J. Braz. Soc. Mech. Sci.* **2000**, *22*, 457.
29. Gazonas, G. A.; Ford, J. C. *Exp. Mech.* **1992**, *6*, 154.
30. Duffy, K. P.; Mellor, A. M. *J. Propul. Power* **1993**, *9*, 377.
31. Wang, J.; Kang, Y. L.; Qin, Q. H.; Fu, D. H.; Li, X. Q. *Comp. Mater. Sci.* **2008**, *43*, 1160.
32. Palmer, S. J. P.; Field, J. E.; Huntley, J. M. *Proc. R. Soc. A* **1993**, *440*, 399.
33. Hufferd, W. L.; Francis, E. C. Failure Theory Evaluation with Analog Devices; JANNAF CPIA Publication: New York, **1982**; p 95.
34. Hinterhoelzl, R. M.; Schapery, R. A. *Mech. Time Depend Mater.* **2004**, *8*, 65.
35. Swanson, S. R.; Christensen, L. W. *J. Spacecraft Rockets* **1983**, *20*, 559.
36. Duncan, E. J. S.; Margetson, J. *Propellants Explosives Pyrotechnics* **1998**, *23*, 94.
37. Xu, J. S.; Chen, X.; Wang, H. L.; Zheng, J.; Zhou, C. S. *Int. J. Solids Struct.* **2014**, *51*, 3209.
38. Wang, X.; Ma, S. P.; Zhao, Y. T.; Zhou, Z. B.; Chen, P. W. *Polym. Test.* **2011**, *30*, 861.
39. Park, S. W.; Schapery, R. A. *Int. J. Solids Struct.* **1997**, *34*, 931.
40. Lundstrom, R.; Ekblad, J. *Annial. Trans. Nordic. Rheol. Soc.* **2006**, *14*, 227.
41. Sultana, S.; Bhasin, A.; Liechti, K. M. *Constr. Build. Mater.* **2014**, *53*, 604.